Continuous quantum phase transition between two topologically distinct valence bond solid states associated with the same spin value

Dong Zheng, Guang-Ming Zhang, Tao Xiang, and Dung-Hai Lee

Phys. Rev. B **83**, 014409 — Published 13 January 2011

DOI: 10.1103/PhysRevB.83.014409

Continuous quantum phase transition between two topologically distinct valence bond solid states associated with the same spin value

Dong Zheng[1], Guang-Ming Zhang[1], Tao Xiang[2,3], and Dung-Hai Lee[4,5]
[1]*Department of Physics, Tsinghua University, Beijing, 100084, China*
[2]*Institute of Physics, Chinese Academy of Sciences, Beijing 100190, China;*
[3]*Institute of Theoretical Physics, Chinese Academy of Sciences, Beijing 100190, China*
[4]*Department of Physics, University of California at Berkeley, Berkeley, CA 94720, USA*
[5]*Material Science Division, Lawrence Berkeley National Laboratory, Berkeley, CA 94720, USA*
(Dated: December 1, 2010)

We propose a one-dimensional quantum Heienberg spin-2 chain, which exhibits two topologically distinct valence bond solid states in two different solvable limits. We then construct the phase diagram and study the quantum phase transition between these two states using the infinite time evolving block decimation algorithms. From the scaling relation between the entanglement entropy and correlation length, we determine that the central charge for the underlying critical conformal field theory is $c = 2$.

PACS numbers: 05.30.-d, 03.65.Fd, 64.60.-i

I. INTRODUCTION

Recently there have been considerable interests in the investigations of topological ordered states, and the quantum phase transitions between them. Since topological ordered phases usually do not exhibit conventional symmetry breaking, these phase transitions naturally can not be described by the conventional Landau-Ginzburg paradigm. Despite of the lack of local order parameters, tremendous progresses have been made in characterizing topological ordered states. Properties such as ground state degeneracy, quasiparticle statistics, existence of edge states, topological entanglement entropy,[1,2] and entanglement spectrum[3] have been proposed and used to distinguish different topological ordered states. In contrast, the study of topological phase transitions is still in its infancy, and progresses are in demand.

One dimensional quantum spin chains have been a subject of interests for many years. It started with the famous Haldane conjecture,[4] followed by the Affleck-Kennedy-Lieb-Tasaki (AKLT) construction of the valence bond solid (VBS) states and their associated parent Hamiltonians.[5] Moreover, the SU(2) AKLT model has been generated by introducing q-deformed SU(2) group,[6] supersymmetry,[7] and higher symmetric groups, such as SU(n),[8] SP(n),[9], and SO(n).[10] More recently a systematic method for constructing translational invariant VBS state for the general Lie group has been proposed.[11]

For the $S = 1$ VBS state, there is an appealing physical picture where each spin-1 is decomposed into two "virtual" spin-1/2's. Across each valence bond, two neighboring virtual spins pair into a singlet. den Nijs and Rommelse proposed a nonlocal string order parameter (SOP) which revealed a hidden "diluted antiferromagnetic order".[12] Kennedy and Tasaki found an unitary transformation that turns the nonlocal SOP to a local ferromagnetic order parameter associated with a hidden $Z_2 \otimes Z_2$ symmetry.[13] However, it is extremely difficult to generalize such a description to the cases of higher quantum integer spin chains.

In this paper, we present a model for the $S = 2$ chain which exhibits two distinct VBS states in different parameter regimes. For one of the states, each spin-2 is decomposed into two virtual spin-1's, and for the other it is decomposed into two spin-3/2's. These virtual spins then pair up across every nearest neighbor bonds. In the following, we shall refer to these two states as VBS_1 and $\text{VBS}_{3/2}$ states. For an open chain, the ground states have 9- and 16-fold degeneracies in these two cases, respectively. Hence these two VBS states have different topological order. Interestingly, there is a continuous quantum phase transition between these two VBS states. By analyzing the relation between the von Neumann entanglement entropy and the spin-spin correlation length,[14,15] we deduce the central charge associated with the critical conformal field theory to be two. We further conjecture that the underlying critical field theory may be described by the level-four $SU(2)$ Wess-Zumino-Witten model.

The paper is organized as follows. In Sec. II, we review the properties of VBS_1 and $\text{VBS}_{3/2}$ states. In Sec. III, the quantum phase transition for the above $S = 2$ spin model is explored using the infinite time evolving decimation method.[16] The entanglement spectrum around the phase transitions is studied and the central charges for the underlying conformal field theory at the critical line are determined. A summary is given in Sec. IV.

II. TWO DISTINCT VBS STATES OF A SPIN-2 CHAIN

The model Hamiltonian of the spin-2 chain is proposed as

$$\begin{aligned} H &= \sum_i \left[J_2 P_2(i,i+1) + J_3 P_3(i,i+1) + P_4(i,i+1)\right] \\ &= \sum_i \Big[\frac{189J_3 - 400J_2 + 30}{420}(\mathbf{S}_i\mathbf{S}_{i+1}) \\ &\quad - \frac{40J_2 + 7J_3 - 9}{360}(\mathbf{S}_i\mathbf{S}_{i+1})^2 \\ &\quad + \frac{10J_2 - 5J_3 + 1}{180}(\mathbf{S}_i\mathbf{S}_{i+1})^3 \\ &\quad + \frac{20J_2 - 7J_3 + 1}{2520}(\mathbf{S}_i\mathbf{S}_{i+1})^4\Big]. \end{aligned} \tag{1}$$

where $P_T(i,i+1)$ is the SU(2) symmetric operator that projects the spin states associated with sites i and $i+1$ into the total spin-T multiplet. The coupling constants J_2 and J_3 are all positive. In order to make the paper self-contained, we first review the VBS_1 and $\text{VBS}_{3/2}$ states, respectively.

A. The VBS_1 state - AKLT state

To construct this state, we view each spin-2 as a symmetric product of two virtual spin-1's. In the VBS_1 state, two neighboring virtual spin-1 form a singlet. The direct product of the spin-2 multiplets on neighboring sites can be decomposed into a direct sum of the total spin $S=0,1,2,3,4$ multiplets. Due to the singlet pairing of the neighboring virtual spin-1's, the total spin $S=3,4$ multiplets can not be generated. For $J_2=0$, the model Hamiltonian only penalizes the $S=3,4$ two-spin states. Hence VBS_1 state is the unique ground state of Eq.(1). In an open chain, the unpaired virtual spin-1's at the two ends are free, and they give rise to the $3\times 3=9$ fold ground state degeneracy.[5,13]

In order to write down the ground state wave function, we can use the Schwinger boson representation, and the spin-2 operators can be expressed as

$$S_i^+ = a_i^\dagger b_i,\ S_i^- = b_i^\dagger a_i,\ S_i^z = (a_i^\dagger a_i - b_i^\dagger b_i)/2, \tag{2}$$

with a local constraint $a_i^\dagger a_i + b_i^\dagger b = 4$. Then the $S=2$ AKLT VBS ground states can be expressed in a simple form,[17]

$$|\Psi_{\text{AKLT}}\rangle = \prod_i (a_i^\dagger b_{i+1}^\dagger - b_i^\dagger a_{i+1}^\dagger)^2 |vac\rangle \tag{3}$$

where each $\left(a_i^\dagger b_{i+1}^\dagger - b_i^\dagger a_{i+1}^\dagger\right)$ creates a singlet bond composed of two spin-$1/2$ between i and $i+1$ sites. Furthermore, by re-arranging the creation operators in Eq.(3) and combining operators with the same site operators together, $|\Psi_{\text{AKLT}}\rangle$ can be written in a matrix product state form straightforwardly,

$$|\Psi_{\text{AKLT}}\rangle = \sum_{i_1,i_2,\cdots,i_N=-2}^{2} \text{Tr}(A^{[i_1]}A^{[i_2]}\cdots A^{[i_N]})|i_1 i_2\cdots i_N\rangle, \tag{4}$$

where $\left\{A^{[m]}\right\}$ with $m=\pm 2,\pm 1,0$ are 3×3 matrixes,

$$A^{[-2]} = \begin{pmatrix} 0 & 0 & 0 \\ 0 & 0 & 0 \\ 2\sqrt{6} & 0 & 0 \end{pmatrix},\ A^{[-1]} = \begin{pmatrix} 0 & 0 & 0 \\ -2\sqrt{3} & 0 & 0 \\ 0 & 2\sqrt{3} & 0 \end{pmatrix},$$
$$A^{[0]} = \begin{pmatrix} 2 & 0 & 0 \\ 0 & -4 & 0 \\ 0 & 0 & 2 \end{pmatrix},\ A^{[1]} = \begin{pmatrix} 0 & 2\sqrt{3} & 0 \\ 0 & 0 & -2\sqrt{3} \\ 0 & 0 & 0 \end{pmatrix},$$
$$A^{[2]} = \begin{pmatrix} 0 & 0 & 2\sqrt{6} \\ 0 & 0 & 0 \\ 0 & 0 & 0 \end{pmatrix}. \tag{5}$$

B. The $\text{VBS}_{3/2}$ State - SO(5) symmetric state

Instead of splitting a spin-2 into two virtual spin-1's, one can also split it into two spin-$3/2$'s. In the following, we shall first view the $\text{VBS}_{3/2}$ state as the AKLT state of a larger symmetry group, which is equivalent to the $SO(5)$ symmetric matrix product state in a two-leg electronic ladder[18]. Afterwards we will rephrase everything in terms of the physical spin $SU(2)$. As pointed out in Ref.[19], one can view the $\pm 3/2,\pm 1/2$ states of a spin-3/2 as the four states of the spinor representation of $SO(5)$. Similarly one can regard the $\pm 2,\pm 1,0$ states of spin-2 as the five-dimensional vector irreducible representation (IR) of $SO(5)$. Analogous to decomposing a spin-1 vector IR of $SU(2)$ into two virtual spin-$1/2$'s spinor IR of $SU(2)$, we can view the vector IR as the symmetric component of the tensor product of two virtual spinor IR's, i.e.,

$$\underline{4}\otimes\underline{4} = \underline{1}\oplus\underline{5}\oplus\underline{10}. \tag{6}$$

The numerals are the dimensions of the $SO(5)$ IR's. The tensor product of two $\underline{5}$'s on adjacent sites decomposes into

$$\underline{5}\otimes\underline{5} = \underline{1}\oplus\underline{10}\oplus\underline{14}. \tag{7}$$

Comparing expressions of Eq.(6) and Eq.(7), we view Eq. (6) as the tensor product of two neighboring virtual spins after their respective partners have form $SO(5)$ singlet with other virtual spins. Then one can find that $SO(5)$ singlet $\underline{1}$ and the antisymmetric $\underline{10}$ appear in the decomposition but the symmetric $\underline{14}$ is absent. Therefore, if $H=\sum_i P_{14}(i,i+1)$, the $\text{VBS}_{3/2}$ state where neighboring virtual $\underline{4}$'s pair into $SO(5)$ singlet will be the ground state. In an open chain, due to the unpaired free $SO(5)$ spinors at two ends, the ground states are $4\times 4=16$ fold degenerate. A clear and detailed argument of this degeneracy is given is section III(B). Furthermore, the projection operator $P_{\underline{14}}(i,i+1)$ can be expressed in terms of the $SO(5)$ generators[10]

$$P_{\underline{14}}(i,j) = \frac{1}{2}\sum_{1\le a<b\le 5} L_i^{ab}L_j^{ab} + \frac{1}{10}\Big(\sum_{1\le a<b\le b} L_i^{ab}L_j^{ab}\Big)^2 + \frac{1}{5}. \tag{8}$$

Because the physical spin is $SU(2)$, which is a subgroup of $SO(5)$, each IR of $SO(5)$ must decompose into an integral number of $SU(2)$ multiplets. Thus the $\underline{14}$ discussed above must be expressible as the direct sum of $SU(2)$ IR obtained by decomposing the direct product of two $S=2$ multiplets. Since the 14-dimensional IR is symmetric upon the exchange of site indices, it must only contain even-spin $SU(2)$ multiplets. A simple calculation shows that $\underline{14}\to S=2\oplus S=4$. Consequently, $\sum_i P_{14}(i,i+1)$ reduces to Eq.(1) with $J_3=0$, which is first given by Tu, Zhang, and Xiang.[10]

Moreover, the $SO(5)$ generators can be represented by $L^{ab}=\sum_{\alpha,\beta}\psi_\alpha^\dagger\Gamma_{\alpha\beta}^{ab}\psi_\beta$, where $\psi_{j,\alpha}^\dagger$ creates a spin-$3/2$ fermion with spin index $\alpha=\pm 3/2,\pm 1/2,\Gamma^a,(a=1,\cdots,5)$ are the 4-dimensional Dirac Γ matrices, and $\Gamma^{ab}=\frac{i}{2}[\Gamma^a,\Gamma^b]$. By using the above representations, the $\text{VBS}_{3/2}$ state can be

written as[10]

$$|\mathrm{VBS}_{3/2}\rangle = \prod_j \mathcal{P}_{S=2}(j)(\sum_{\alpha\beta} \psi^\dagger_{j,\alpha}\mathcal{R}_{\alpha\beta}\psi^\dagger_{j+1,\beta})|\mathrm{vac}\rangle \quad (9)$$

where $\mathcal{P}_{S=2}(j)$ is the spin-quintet projector and $\sum_{\alpha\beta}\psi^\dagger_{j,\alpha}\mathcal{R}_{\alpha\beta}\psi^\dagger_{j+1,\beta}$ is an $SO(5)$ invariant valence bond singlet creation operator. $\mathcal{R}$ is the $SO(5)$ invariant matrix. This $\mathrm{VBS}_{3/2}$ state can also be expressed as a matrix product states (MPS)

$$|\mathrm{VBS}_{3/2}\rangle = \sum_{i_1,..,i_N=-2}^{2} \mathrm{Tr}(B^{[i_1]}B^{[i_2]}\cdots B^{[i_N]})|i_1 i_2 \cdots i_N\rangle, \quad (10)$$

where $\{B^{[m]}\}$ with $m = 0, \pm1, \pm2$ are given by the following 4×4 matrices

$$B^{[-2]} = \begin{pmatrix} 0 & 0 & 0 & 0 \\ 0 & 0 & 0 & 0 \\ \sqrt{2} & 0 & 0 & 0 \\ 0 & \sqrt{2} & 0 & 0 \end{pmatrix}, \; B^{[-1]} = \begin{pmatrix} 0 & 0 & 0 & 0 \\ -\sqrt{2} & 0 & 0 & 0 \\ 0 & 0 & 0 & 0 \\ 0 & 0 & \sqrt{2} & 0 \end{pmatrix},$$

$$B^{[0]} = \begin{pmatrix} 1 & 0 & 0 & 0 \\ 0 & -1 & 0 & 0 \\ 0 & 0 & -1 & 0 \\ 0 & 0 & 0 & 1 \end{pmatrix}, \; B^{[1]} = \begin{pmatrix} 0 & \sqrt{2} & 0 & 0 \\ 0 & 0 & 0 & 0 \\ 0 & 0 & 0 & -\sqrt{2} \\ 0 & 0 & 0 & 0 \end{pmatrix}$$

$$B^{[2]} = \begin{pmatrix} 0 & 0 & \sqrt{2} & 0 \\ 0 & 0 & 0 & \sqrt{2} \\ 0 & 0 & 0 & 0 \\ 0 & 0 & 0 & 0 \end{pmatrix}. \quad (11)$$

III. CONTINUOUS QUANTUM PHASE TRANSITIONS

In the model Hamiltonian Eq.(1), for $J_2 = 0$, the ground state of the model is the VBS_1 state,[5] while $J_3 = 0$ it corresponds to the $\mathrm{VBS}_{3/2}$ state.[10] When both J_2 and J_3 are nonzero, the model is no longer exactly solvable. Then, we expect that a quantum phase transition may be reached by adjusting the value of J_3/J_2. To our knowledge, this is one of the few microscopic models, exhibiting continuous quantum phase transitions between two distinct topological ordered phases.

A. Ground state phase diagram

In any one-dimensional quantum spin systems, the corresponding ground states can always be simulated by the wave functions in the MPS form, as the area law can be easily satisfied. To study the ground state properties of the general Hamiltonian Eq.(1), we thus propose a MPS with a finite local matrix dimension to approximate the ground state $|\psi_g\rangle$,

$$|\Psi_g\rangle = \sum_{\cdots m_i m_{i+1}\cdots} \mathrm{Tr}(\cdots\Gamma^{m_i}\Lambda\Gamma^{m_{i+1}}\Lambda\cdots)|\cdots m_i m_{i+1}\cdots\rangle, \quad (12)$$

where $m_i = -2,-1,0,1,2$ is the spin quantum number of S^z_i, $\{\Gamma^{m_i}\}$ is a set of $D\times D$ dimensional matrices with bond dimension D corresponding to number of states kept in density matrix renormalization group, and Λ is also a $D\times D$ dimensional non-negative diagonal matrix with its matrix elements λ_α, satisfying the normalization condition $\sum_\alpha \lambda^2_\alpha = 1$. The trace gives the superposition coefficients of the Hilbert space basis. The local matrices $\{\Gamma^m\}$ and Λ are set to be identical on different sites due to the translation invariance.[20]

The spirit of the infinite time evolving block decimation algorithm (iTEBDA)[16] is to do the following evolution in imaginary time

$$\lim_{\tau\to\infty}\frac{\exp(-H\tau)|\Psi_0\rangle}{\|\exp(-H\tau)|\Psi_0\rangle\|} = \lim_{N\to\infty}\frac{(\exp(-H\varepsilon))^N|\Psi_0\rangle}{\left\|(\exp(-H\varepsilon))^N|\Psi_0\rangle\right\|}, \quad (13)$$

where $|\Psi_0\rangle$ is an arbitrary random initial state having nonzero overlap with $|\psi_g\rangle$, τ is imaginary time, and ε is a small interval satisfying $\varepsilon N = \tau$. It is a projection method with high efficiency: as τ increases, the weight of ground state in evolved state $\exp(-H\tau)|\Psi_0\rangle$ grows exponentially. Next we split the Hamiltonian into two non-commutative parts,

$$H = \sum_{i=\mathrm{odd}}\hat{h}(i,i+1) + \sum_{i=\mathrm{even}}\hat{h}(i,i+1) = H_{odd} + H_{even}, \quad (14)$$

where all the local two-body bond operators $\hat{h}(i,i+1)$ commute with one another in each part H_{odd} or H_{even}. Then Suzuki-Trotter decomposition is used to divide the respective evolution in sequential order,

$$\exp(-H\varepsilon)|\Psi_0\rangle = \exp(-\varepsilon H_{odd})\exp(-\varepsilon H_{even}) + O(\varepsilon^2) \quad (15)$$

Owing to the fact that $\exp(-\varepsilon H_{odd})$ and $\exp(-\varepsilon H_{even})$ compose of commutating evolution operators, all the bond evolution in each part can be implemented simultaneously, which is compatible with the translation invariance of MPS. After each evolution step, the domain of local matrices increases by at least one site and the number of different local matrices increases by a factor at least 5. Then a singular value decomposition and bond dimension truncation are introduced to keep the MPS in the form given by Eq.(12) and bond dimension fixed in each evolution step, the detailed can be found in Ref.[16].

Now we show how to calculate the ground state energy density. First we construct the transfer matrix

$$G = \sum_{m=-2}^{2}\Gamma^m\Lambda\otimes(\Gamma^m)^*\Lambda \quad (16)$$

and compute its dominant eigenvalue η_1, as well as the associated right and left eigenvectors $|r_1\rangle$ and $|l_1\rangle$. Then the matrix used to compute the energy expectation value is constructed as

$$G_E = \sum_{p,q,s,t}\langle p,q|\hat{h}|s,t\rangle\Gamma^p\Lambda\Gamma^q\Lambda\otimes(\Gamma^s)^*\Lambda(\Gamma^t)^*\Lambda. \quad (17)$$

where $\langle p,q|$ and $|s,t\rangle$ are the wave functions defined by local Hilbert space of two adjacent sites and with the spin quantum

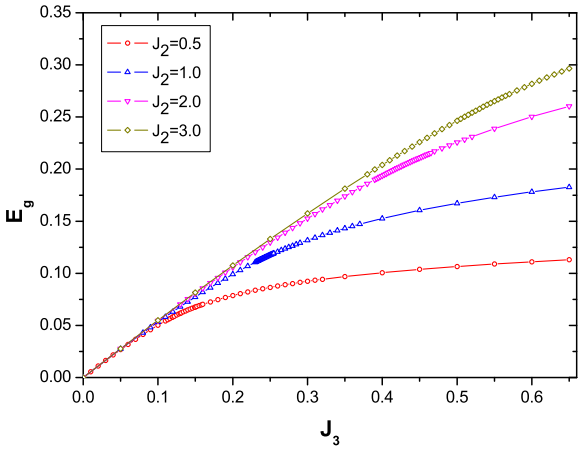

FIG. 1: (Color online) Ground state energy density varies as a function of J_3 for fixed J_2. The local matrix dimension D is set to be 300 in the calculation.

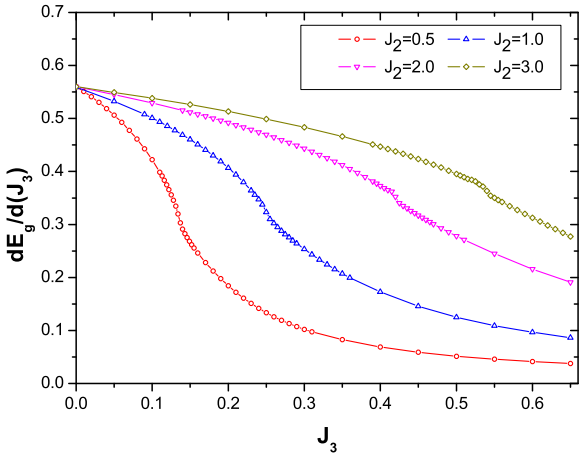

FIG. 2: (Color online) First derivative of the ground state energy density varies as a function of J_3 for fixed J_2.

numbers $p, q, s, t = -2, -1, 0, 1, 2$. The ground state energy per site E_g can be calculated by

$$E_g = \lim_{N\to\infty} \frac{tr\left(G^{N-2}G_E\right)}{tr\left(G^N\right)} = \frac{\langle l_1|G_E|r_1\rangle}{\eta_1^2\langle l_1|r_1\rangle}. \qquad (18)$$

For a fixed J_2, we calculate E_g as a function of J_3. The quantity E_g and its first order derivative with respect to J_3 are finite and continuous, which are displayed in FIG.1 and FIG.2. However, the second derivative of E_g with respect to J_3 exhibits divergence as J_3 is tuned to a certain critical value. This is similar to the specific heat divergence in classical phase transitions. Such a behavior is shown in FIG.3 for several typical values of J_2. We thus conclude that the system undergoes a second-order phase transition at zero temperature. By determining the positions of the critical points, we thus derive the zero temperature phase diagram in FIG.4.

Moreover, the calculations of the spin-spin correlation length and entanglement entropy also show a singular behavior and provide further evidence of the second order phase

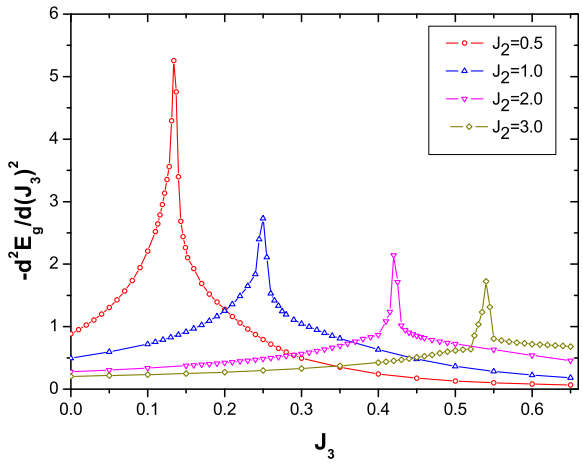

FIG. 3: (Color online) The second order derivative of the ground state energy density varies as a function of J_3 for fixed J_2.

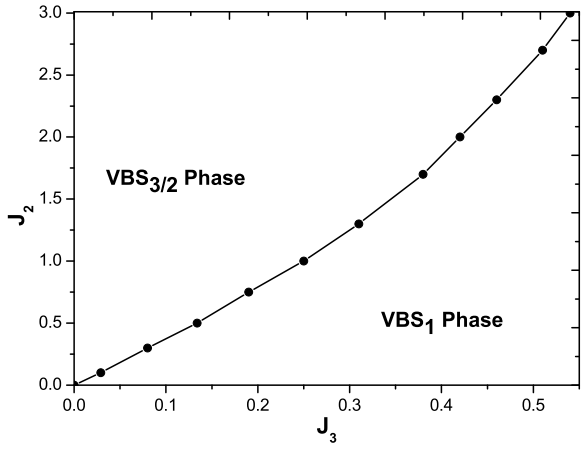

FIG. 4: Ground state phase diagram of the model Hamiltonian Eq.(1).

transition of the model. In FIG.5, the numerical results of both spin-spin correlation length and entanglement entropy are depicted as a function of J_3 for fixed J_2. At the critical point, the spin-spin correlation length is divergent, and the entanglemnt entropy shows a cusp. Away from the critical point, an extrapolation of correlation length and entanglement entropy can be calculated as D goes to infinity, indicating that both of them saturate to finite values. Due to the finite spin-spin correlation length and the form of the model Hamiltonian in terms of projection operators, it is straightforward to prove the existence of excitation gap[21] and to identify two phases separated by the critical line in the $J_2 - J_3$ phase diagram as VBS_1 and $\mathrm{VBS}_{3/2}$ states, respectively. The computational methods of entanglement entropy and correlation length are explained in detail in the following sections.

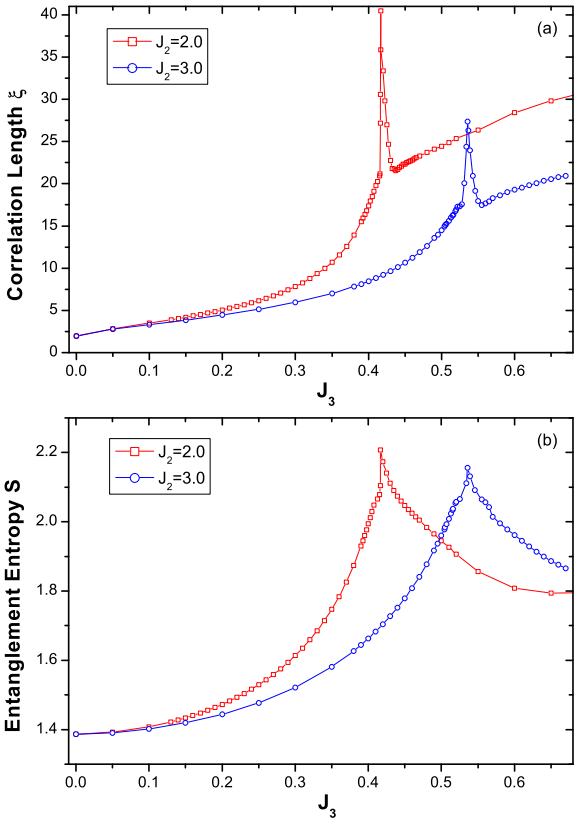

FIG. 5: (Color online) (a) The spin-spin correlation length varies as a function of J_3 for two typical values of J_2. (b) The entanglement entropy varies as a function of J_3 for two typical values of J_2. The local matrix dimension D is fixed at 300 in this calculation.

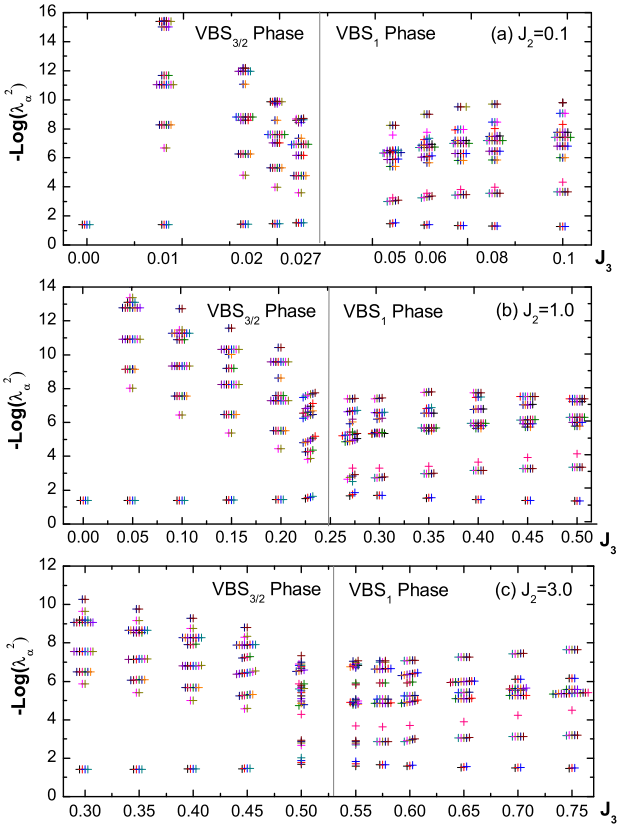

FIG. 6: (Color online) The thirty-sixth lowest values of the entanglement spectra for the $\mathrm{VBS}_{3/2}$ and VBS_1 phases on two sides of the critical points. (a) $(J_2, J_3) = (0.1, 0.029)$, (b) $(J_2, J_3) = (1.0, 0.25)$, (c) $(J_2, J_3) = (3.0, 0.53)$. A light gray vertical line is put on the critical point to separate the two phases. Each entanglement spectrum is represented by a small cross, and the degenerate spectra are spatially staggered a little bit in horizontal direction to distinguish and count them. In this calculations, the local matrix dimension D is set to be 300.

B. Entanglement spectrum across the transition

Li and Haldane[3] have recently proposed that entanglement spectrum (ES), i.e., the minus logarithms of the eigenvalues of a reduced density matrix, can be used to characterize topological order. If there is an entanglement gap separating the low-lying ES and the upper parts, then one can find a one-to-one correspondence between the low-lying ES and the low energy spectrum of individual edge excitations. In particular, the lowest level of the entanglement spectrum for a topological ordered state should be degenerate. When the state changes from $\mathrm{VBS}_{3/2}$ to VBS_1 by tuning the ratio of J_3/J_2, how does the topological order changes in this process, especially when crossing the phase transition point? We will try to use entanglement spectrum as a probe to partially answer this question.

If the MPS in Eq.(12) is in "canonical form", then upon dividing the system into left and right parts the ground state wave function should become

$$|\Psi_g\rangle = \sum_\alpha \lambda_\alpha |\Phi_\alpha^L\rangle |\Phi_\alpha^R\rangle, \tag{19}$$

where $\{|\Phi_\alpha^L\rangle, \alpha = 1, 2, \cdots, D\}$ and $\{|\Phi_\alpha^R\rangle, \alpha = 1, 2, \cdots, D\}$ are orthogonal basis states of the left and right semi-infinite chain,

$$\langle \Phi_\alpha^L | \Phi_\beta^L \rangle = \langle \Phi_\alpha^R | \Phi_\beta^R \rangle = \delta_{\alpha\beta} \tag{20}$$

It can be shown that the canonical condition Eq.(20) imposes the following constraint[22] on the Γ^m and Λ in Eq.(12),

$$\sum_m \Gamma^m \Lambda^2 (\Gamma^m)^\dagger = \sum_m (\Gamma^m)^\dagger \Lambda^2 \Gamma^m = \mathbf{I}_{D^2 \times D^2}. \tag{21}$$

In general, a MPS has a gauge freedom, because the local matrixes can be the same up to a similarity transformation. In canonical form, it is extremely easy and straightforward to write down the entanglement spectra $P_\alpha = -\log(\lambda_\alpha^2)$. In our calculation, we perform the canonical transformation[23] explicitly at the end of iTEBDA and obtain the MPS in its canonical form.

The 36 lowest values of ES are plotted in FIG.6 for $J_2 = 0.1, 1.0$ and 3.0. It can be clearly seen that, for the $\mathrm{VBS}_{3/2}$ state, the lowest entanglement eigenvalue is four-fold degenerate in one to one correspondence with the four-fold degenerate edge states; while for the VBS_1 state, the lowest

eigenvalue of the ES is three-fold degenerate. Above this degenerate eigenvalues there exists a large gap, so the degenerate levels are protected topologically. So such a calculation of the ES can be used to confirm that both VBS_1 and $\mathrm{VBS}_{3/2}$ are really topological ordered states, as well as that the ground state degeneracy of a long enough open chain are really 16 and 9 respectively. When approaching the critical points, the degeneracies are gradually lifted but the gap still survives. However, in the vicinity of quantum critical points $(J_2, J_3) = (0.1, 0.029), (1.0, 0.25), (3.0, 0.54)$, the degeneracies in the ES no longer exist and the large gaps between the degenerate lowest level and the higher levels are no longer present. Due to the expected finite-size effect near the critical region, so far we can not simply conclude that the topological order is destroyed completely at the critical points. Recently a partition with a very non-local real space cut has been proposed[24], and some new light has shed on using ES to detect non-local orders in gapless spin chains. However, it still needs further investigation to clarify this question and will be done in future works.

C. Central charge on the critical line

At the critical points, the system should be described by conformal invariant quantum field theories. For such theories the central charge encodes information about the universality class. According to conformal field theory, the von Neumann entanglement entropy should diverge logarithmically with the correlation length[25],

$$S_e = \frac{c}{6}\ln(\xi) + S_0, \tag{22}$$

where S_e is the entanglement entropy between two semi-infinite parts of a whole chain, c is the central charge, ξ is spin-spin correlation length in units of lattice spacing, and S_0 is a non-universal constant. For a MPS in canonical form, entanglement entropy can be calculated easily[14,15]:

$$S_e = -\sum_{\alpha} \lambda_\alpha^2 \ln \lambda_\alpha^2 \tag{23}$$

where λ_α are the coefficients in Eq.(19).

The spin correlation length can be deduced by two points spin-spin correlation function as

$$\begin{aligned}\lim_{|i-j|\to\infty}\lim_{N\to\infty}\langle S_i^z S_j^z\rangle &= \lim_{|i-j|\to\infty}\lim_{N\to\infty}\frac{tr\left(G^{N-|i-j|-1}G_z G^{|i-j|-1}G_z\right)}{tr\left(G^N\right)} \\ &= \lim_{|i-j|\to\infty}\frac{|\langle l_1|G_z|r_1\rangle|^2}{\eta_1^2\langle l_1|r_1\rangle} + \frac{\langle l_1|G_z|r_2\rangle\langle l_2|G_z|r_1\rangle}{\eta_1\eta_2\langle l_1|r_1\rangle}\left(\frac{\eta_2}{\eta_1}\right)^{|i-j|}\end{aligned} \tag{24}$$

where transfer matrix G, eigenvalues η_1, and eigenvectors $\langle l_1|$ and $|r_1\rangle$ have the same definition as in Eq.(16). η_2 is the second largest magnitude eigenvalue of G and $\langle l_2|$ and $|r_2\rangle$ are corresponding left and right eigenvectors. Similar to G_E in Eq.(17), G_z is defined by

$$G_z = \sum_{p,q}\langle p|\hat{S}^z|q\rangle \Gamma^p\Lambda\otimes(\Gamma^q)^*\Lambda. \tag{25}$$

Generally, for a state without spin long-range order, $\langle l_1|G_z|r_1\rangle = 0$, the two points correlation function can be written as

$$\lim_{|i-j|\to\infty}\lim_{N\to\infty}\langle S_i^z S_j^z\rangle \sim e^{-\frac{|i-j|}{\xi}}, \tag{26}$$

where the correlation length $\xi = 1/\log(|\eta_1/\eta_2|)$.

Using Eq.(23) we have calculated S_e and ξ in the vicinity of several different critical points on the phase boundary of FIG.4. The associated scaling relation between S_e and ξ are shown in FIG.7. Although there may be some deviations at small ξ, S_e tends to lie on the $c = 2$ line for large ξ. The fact that all the central charges are approximately equal to 2 implies a single fixed point governing the critical behavior of the entire phase transition line. So far the conformal field theory with $c > 1$ can not be classified systematically, and therefore to determine the corresponding conformal field theory of a fixed line with $c = 2$ might be worth attempting.

Here we present some conjectures deduced from the conformal field theory kinematics. According to the central charge value and the constituents of the VBS_1 and $\mathrm{VBS}_{3/2}$ states, the level-four SU(2) Wess-Zumino-Witten model is the most possible effective field theory and the conformal weight of the primary field given by[26] $\Delta^{(j)} = j(j+1)/6$ with $j = 0, 1/2, 1, 3/2, 2$. Actually, the level-four $SU(2)$ Wess-Zumino-Witten model can be regarded as the effective critical field theory of the following spin $S = 2$ antiferromagnetic

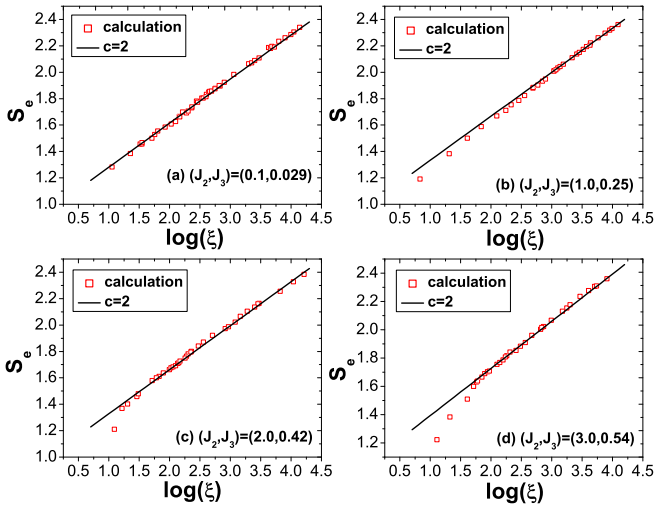

FIG. 7: (Color online) The scaling behavior of the entanglement entropy S_e as the correlation length ξ in the vicinity of different critical points. (a) $(0.1, 0.029)$, (b) $(1.0, 0.25)$, (c) $(2.0, 0.42)$, (d) $(3.0, 0.54)$. The black solid line is as a reference with a central charge $c = 2$ and the red squares are numerical results. In our calculation, the local matrix dimension increases from 12 to 600.

Takhtajan-Babujian model[27]:

$$H = J\sum_i \left[-\frac{1}{4} + \frac{13}{48}(\mathbf{S}_i\mathbf{S}_{i+1}) + \frac{43}{864}(\mathbf{S}_i\mathbf{S}_{i+1})^2 - \frac{5}{432}(\mathbf{S}_i\mathbf{S}_{i+1})^3 - \frac{1}{288}(\mathbf{S}_i\mathbf{S}_{i+1})^4\right], \quad (27)$$

which can be written in terms of the projection operators as

$$H = J\sum_i [J_1P_1(i,i+1) + J_2P_2(i,i+1) + J_3P_3(i,i+1) + P_4(i,i+1)] \quad (28)$$

with $J_1 = \frac{12}{25}$, $J_2 = \frac{18}{25}$ and $J_3 = \frac{22}{25}$.

Compared to the model Hamiltonian Eq.(1), there appears an additional interaction term $P_1(i, i+1)$ with the largest interaction strength $J_1 = \frac{12}{25}$. By calculating the entanglement spectrum, we find that this critical point just lies on the boundary between the AKLT and a dimerization phases. For the dimerization phase, the entanglement spectrum show an even-odd difference from the topological ordered phase, i.e., if the bipartition is done at a bond connecting left even and right odd sites, the lowest spectrum is 5 fold degenerate, otherwise the lowest spectrum is non-degenerate and has a big gap with the upper part. This even-odd difference indicates the existence of dimerization phase. The relation between this critical point and the $SO(5)$-AKLT critical line can be understood as follows. When we fix $J_1 = \frac{12}{25}$ and $J_2 = \frac{18}{25}$, J_3 varies from 0 to $\frac{22}{25}$, the system evolves from the $SO(5)$ symmetric phase to the dimerization phase, and then the AKLT phase for $J_3 > \frac{22}{25}$. Moreover, for the fixed value of J_2 the dimerization region shrinks and finally disappears when J_1 is decreased, which is compatible with our ground state phase diagram. Therefore, we expect that there exists a crossover flow from the fixed line of the transition between the $SO(5)$-AKLT phases to the $S = 2$ antiferromagnetic Takhtajan-Babujian model.

IV. CONCLUSION

In summary, we propose a one-dimensional spin-2 Hamiltonian, which exhibits two topologically distinct VBS states in different solvable limits. By using the infinite time evolving block decimation algorithms, we have studied the quantum phase transition between them and determined the central charge to be $c = 2$. Of course, continuous phase transition between topological phases characterized by different number of edge states is known. For example, by tuning the coefficient of the topological term in the $SO(3)/SO(2)$ non-linear σ model, it is possible to induce phase transition between VBS states associated with *different spin values*. The transition studied in this paper is very different. It takes place between two topologically distinct VBS states associated with the *same* spin value. We are not aware of any previous study of this type of phase transition.

Acknowledgments

The authors are grateful to Dr. Hong-Hao Tu for stimulating discussions and earlier collaborations. We acknowledge the support of NSF of China and the National Program for Basic Research of MOST-China. DHL was supported by DOE grant number DE-AC02-05CH11231.

Note Added After we submitted the original version of this manuscript for publication, a paper[28] concerning with the similar issue by different numerical density matrix renormalization group method on a finite length of chain appeared on the archive, where the authors claimed the existence of dimerization phase separated the VBS_1 and $\mathrm{VBS}_3/2$ phases in the ground state phase diagram. However, if the ground state energy density and its second-order derivative do not show any singularity as the coupling parameters approach to the boundary of the "dimerization phase" on both sides, no quantum phase transition can occur, and the claim of dimerization phase existence is not reliable.

[1] A. Kitaev, J. Preskill, Phys. Rev. Lett. **96**, 110404 (2006).
[2] M. Levin and X. G. Wen, Phys. Rev. Lett. **96**, 110405 (2006).
[3] H. Li and F. D. Haldane, Phys. Rev. Lett. **101**, 010504 (2008).
[4] F. D. M. Haldane, Phys. Lett. A **93**, 464 (1983); Phys. Rev. Lett. **50**, 1153 (1983).
[5] I. Affleck, T. Kennedy, E. H. Lieb, and H. Tasaki, Phys. Rev. Lett. **59**, 799 (1987); Commun. in Math. Phys. **115**, 477 (1988).
[6] A. Klumper, A. Schadschneider, and J. Zittartz, J. Phys. A **24**, L955 (1991); K. Totsuka and M. Suzuki, J. Phys. A **2**7, 6443 (1994).
[7] D. Arovas, K. Hasebe, X. L. Qi, and S. C. Zhang, Phys. Rev. B **79**, 224404 (2009).
[8] I. Affleck, D. Arovas, J. Marston, and D. Rabson, Nucl. Phys. B **366**, 467 (1991); M. Greiter, S. Rachel, and D. Schuricht, Phys. Rev. B **75**, 60401 (2007); D. Arovas, Phys. Rev. B **77**, 104404 (2008).
[9] D. Schuricht and S. Rachel, Phys. Rev. B **78**, 014430 (2008).
[10] H.-H. Tu, G.-M. Zhang, T. Xiang, Phys. Rev. B **78**, 094404 (2008); J. Phys. A: Math. Theor. **41**, 415201 (2008).
[11] H.-H. Tu, G.-M. Zhang, T. Xiang, Z.-X. Liu, and T.-K. Ng, Phys. Rev. B **80**, 014401 (2009).
[12] M. den Nijs and K. Rommelse, Phys. Rev. B **40**, 4709 (1989).
[13] T. Kennedy and H. Tasaki, Phys. Rev. B **45**, 304 (1992); M. Oshikawa, J. Phys. Condens. Matter **4**, 7469 (1992).
[14] L. Tagliacozzo, T. R. de Oliverira, S. Iblisdir, and J. I. Latorre, Phys. Rev. B **78**, 024410 (2008).
[15] F. Pollmann, S. Mukerjee, A. M. Turner, J. E. Moore, Phys. Rev. Lett. **102**, 255701 (2009).
[16] G. Vidal, Phys. Rev. Lett. **98**, 070201 (2007).
[17] D. P. Arovas, A. Auerbach, and F. Haldane, Phys. Rev. Lett. **60**, 531 (1988).
[18] D. Scalapino, S. C. Zhang, and W. Hanke, Phys. Rev. B **58**, 443 (1998).
[19] C. J. Wu, J. P. Hu, S. C. Zhang, Phys. Rev. Lett. **91**, 2003 (186402).
[20] Here we just give an illustration of how to do iTEBD numerical simulation. In actual calculations, an artificial two-fold translational invariance is introduced in the MPS, as the local Hamiltonian includes the nearest neighbor two-body interactions only.
[21] M. B. Hastings and T. Koma, Comm. Math. Phys. **265**, 781 (2006).
[22] D. Perez-Garcia, F. Verstraete, M. M. Wolf, J. I. Cirac, Quantum Inf. Comput. **7**, 401 (2007).
[23] R. Orus and G. Vidal, Phys. Rev. B **78**, 155117 (2008).
[24] R. Thomale, D. P. Arovas, B. A. Bernevig, Phys. Rev. Lett. **105**, 116805 (2010).
[25] P. Calabrese and J. Cardy, J. Stat. Mech.: Theory Exp. (2004) P06002; Int. J. Quantum Inf. **4**, 429 (2006).
[26] A. B. Zamolodchikov and V. F. Fateev, Sov. Phys. JETP **43**, 657 (1986).
[27] L. A. Takhtajan, Phys. Lett. **87A**, 479 (1982); H. M. Babujian, Phys. Lett. **90A**, 479 (1982); F. C. Alcaraz and M. J. Martins, J. Phys. A **21**, 4397 (1988).
[28] J. Zang, H. C. Jiang, Z. Y. Weng, and S. C. Zhang, arXiv:1002.0966, Phys. Rev. B **81**, 224430 (2010).